Climate Dynamics (1996) 12:701–709

Climate Dynamics

High frequency pulses of East Asian monsoon climate in the last two glaciations: link with the North Atlantic

Z. Guo[1], T. Liu J. Guiot[2], N. Wu[1], H. Lü[1], J. Han J. Liu[1], Z. Gu[1]

[1] Institute of Geology, Chinese Academy of Sciences, PO Box 9825, Beijing 100029, China
[2] Laboratoire de Botanique Historique et Palynologie, UA CNRS 1152, Faculté de St-Jérôme, Marseille F-13397 Cédex 20

Received: 16 October 1995 / Accepted: 10 May 1996

Abstract. Three loess sections in the Loess Plateau of China have been studied to characterize the variations of the East Asian monsoon climate in the Late Quaternary period. Paleo-weathering profiles based on two weathering indices reveal a series of spatially correlative intervals of lower weathering intensity (LW), in the last glacial and late penultimate glacial loess, indicating significantly cooler or/and drier conditions. Most of them are identified at or near the transitional boundaries between loess and soil units, suggesting that climatic conditions favorable for LW events tended to occur at or near major climatic boundaries. Twenty-eight radiocarbon and thermoluminescence measurements, combined with Kukla祖 magnetic susceptibility age model date these events at ∼ 14, ∼ 21, -29, -38, -52, -71, ∼ 135, and ∼ 145 ka BP, with ∼ 5-10 ka frequency inlaid within the orbitally induced -20-ka periodicity. The ages of the first six events in the last glacial period are therefore close to those of the coarse-grained Heinrich layers in the North Atlantic Ocean, which resulted from massive discharges of icebergs. The results indicate that the climate in the area affected by the East Asian monsoon has experienced high-frequency changes more or less synchronous with the Heinrich events. These high-frequency changes have been reported by Porter and An, based on the grain-size time series from the Luochuan loess section. Our data also reveal that similar events also occurred during the penultimate glaciation. The mechanisms linking the Heinrich events and the East Asian monsoon climate may be similar to that driving the Younger Dryas event which has been identified in a large number of records in China and in the surrounding oceans.

Correspondence to: Z. T. Guo

1 Introduction

The Quaternary soil-loess sequences in the Loess Plateau of China provide complete and continuous records of East Asian monsoon climate (Liu 1985; Kukla 1987; Liu and Ding 1993; Liu et al. 1993; Ding et al. 1994). This is particularly true for the sequence from the last climatic cycle (An et al. 1991; Beer et al. 1993; Liu et al. 1995). The modern climate in the region is mainly driven by two alternative monsoons (Zhang and Lin 1987), i.e., the warm-humid southeast summer monsoon leading to abundant precipitation in summer; and the cold-dry northwest winter monsoon responsible for dust storms in winter and early spring (Liu 1985; An et al. 1993). Numerical experiments (Ruddiman et al. 1989; Manabe and Broccoli 1990) suggested that the initiation of monsoon climate in Asia might be associated with orographic uplift of the Himalayas and of the Tibetan Plateau which can be traced back to the pre-Quaternary era (Turner et al. 1993), as seems consistent with geological evidence of the monsoons (Liu and Ding 1993). The soil-loess sequence is therefore commonly interpreted as indication of alternating waxings and wanings of the summer and winter paleomonsoons where the soil-forming periods correspond to strengthened summer monsoon and loess deposition correspond to strengthened winter monsoon (An et al. 1991; Liu et al. 1995; Maher et al. 1994). Loess deposition and pedogenesis are, indeed, competing processes at all times, and the presence of a paleosol simply indicates that the latter process was predominant (An et al. 1991; Guo et al. 1991; Verosub et al. 1993).

Many of the earlier studies on loess were mainly centered on the long-term evolution and major climatic events attributable to planetary orbital or ice-sheet forcing (An et al. 1991; Ding et al. 1994; Liu et al. 1995; Guo et al. 1996). Several studies (Zhou et al. 1991; An et al. 1993), however, indicate that the temporal resolution of the soil-loess sequences is sufficient to record climatic events of much shorter duration. In recent years, studies in the North Atlantic (Heinrich 1988; Broecker et al. 1992; Bond et al. 1992, 1993) and

Greenland (Dansgaard et al. 1993) have demonstrated that rapid, high-amplitude climatic changes have been recorded in deep-sea sediments and in ice cores. Determination of the geographic extent of these changes is crucial for an understanding of the mechanisms driving these changes. Our question asks to what degree are these rapid events recorded in loess and in other climate-related records of China

A correlation between the Luochuan loess section in China and the Heinrich events in North Atlantic has been proposed by Porter and An (1995). Based on a study of paleo-weathering intensity of three loess sections in the Loess Plateau region and our published dating results, this work attempts to study (1) whether these climatic signals have been documented by other climate proxies from other localities; and (2) whether similar signals exist in the late penultimate glacial loess.

2 **General setting and methods**

The three sections studied are located, from the southernmost to the northern part of Loess Plateau, at Weinan (34°20 惟, 109°30 悳), Luochuan (upper Heimugou section, 35°45 惟, 109°25 悳) and Yichuan (36°03 惟, 110°10 悳) and all of them are in the Shaanxi Province (Fig. 1). The studied portion of the loess sequence involves the Holocene soil at the top (SO) (Fig. 2); the Malan loess (L1); the soil complex of the Last Interglacial (S1); and the upper part of the penultimate glacial loess unit (L2). The middle part of the Malan loess (L1) contains a weak soil complex usually referred to as L1SS1 (Kukla and An 1989). At Weinan, it can be defined as two soils intercalated by a thin loess layer. The S1 soil at Weinan consists of three subsoil units (Liu et al. 1995). The upper part (34 cm at Weinan; 50 cm at Luochuan; and 80 cm at Yichuan) of the SO soil at the three sites has been disturbed by agricultural activities, and only the lower part is undisturbed, as is confirmed by micromorphological observations.

Magnetic susceptibility has proven particularly useful in characterizing the stratigraphic boundaries of soil-loess sequences in China (Kukla et al. 1988; Kukla and An 1989). The susceptibility signal is usually greater in soils than in the over- and underlying loess. To ensure an accurate stratigraphic correlation of the studied sections, magnetic susceptibility is measured on dry samples taken at 10 cm intervals using a Bartington susceptibility meter and is expressed in SI units (Fig. 2).

To assess the weathering intensity, samples were taken at 10 cm intervals representing an approximate average temporal resolution of -750-800 years for Malan loess (L1) and -1800-2100 y for SO and S1 soils, based on published chrono-stratigraphic studies (Kukla et al. 1988; Liu et al. 1995). We use two indices of weathering:

1. The chemical index of weathering (CIW) defined by Harnois (1988), as CIW = $Al_2O_3*100/(Al_2O_3 + CaO + Na_2O)$ (molecular proportions), is a measurement of the proportion of Al_2O_3 versus the labile oxides in the samples. The CIW is calculated based on the data of chemical composition analyzed by X-ray fluorescence using a Philips PW-1400 unit. To eliminate the effect of dissolution and reprecipitation of calcium carbonate on the CIW values, carbonate content is measured in order to calibrate the X-ray fluorescence data. The calibrated results represent the chemical composition of non-calcareous material and are used to calculate CIW.

2. The Fed/Fet ratio is a measurement of iron liberated from iron-bearing silicate minerals by chemical weathering to total iron, widely used by European pedologists (Duchaufour 1983). 揊ed is the free iron and is extracted by dithionite-bicarbonate-citrate method (Mehra and Jackson 1960) and is measured

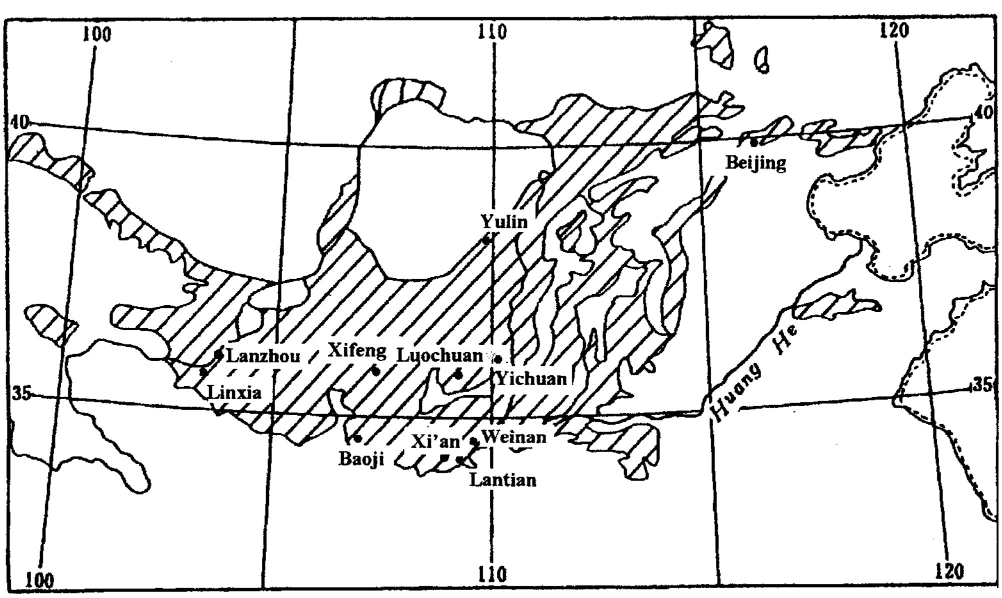

Fig. 1. Map of Chinese Loess Plateau (shaded) and location of the mentioned loess sections (after Kukla and An 1989)

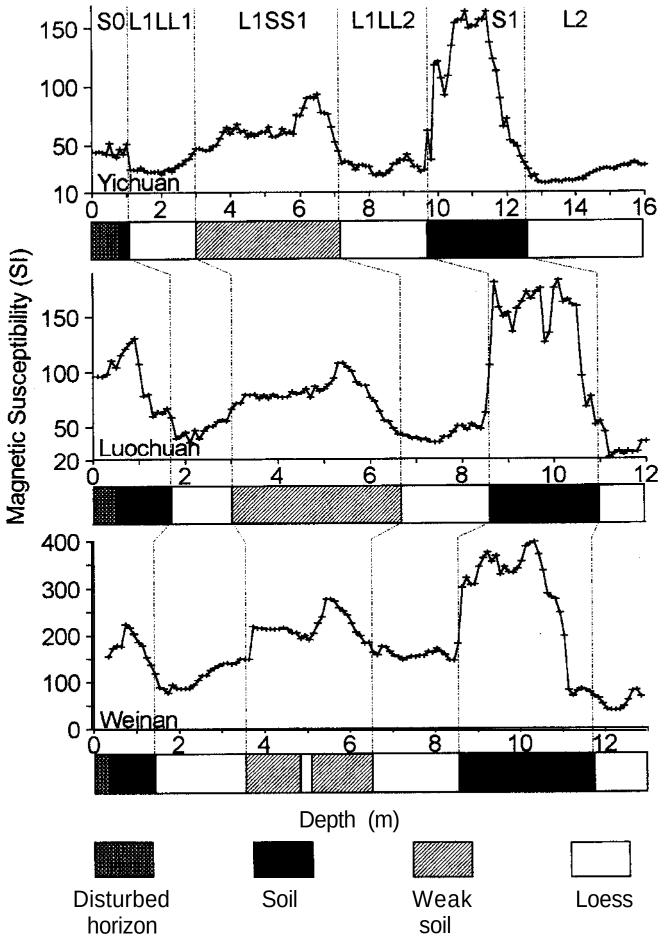

Fig. 2. Stratigraphic correlation of the studied sections based on magnetic susceptibility and lithologic boundaries

spectrophotometrically. The 揊et is the total iron and is measured on acid dissolved samples (McKeygue 1981) by spectrophotometer. The possibility of iron translocation in the L1 loess unit can be basically excluded as no evidence of clay illuviation and hydromorphy features were identified, even in the LlSSl soil.

3 Stratigraphic correlation and time scales

The stratigraphic correlation of the three studied sections is given in Fig. 2. The magnetic susceptibility data provide boundaries that are generally coherent with the lithologic ones identified in the field, except for the lowermost part of the S1 soil complex in the Weinan section. This part of the section corresponds to soil horizons rich in Fe-Mn features attributable to higher soil humidity in which the lower susceptibility values may be explained by pedogenic hydromorphic process affecting the iron minerals responsible for the susceptibility signal (Liu et al. 1995).

The loess sequences of the last climatic cycle are usually dated by radiocarbon and thermoluminescence (TL) measurements (Lu et al. 1988; Kang 1990; Forman 1991; Zhou et al. 1991; Liu et al. 1994; Sun et al. 1995). Correlation with marine $\delta^{18}O$ records (Beer et al. 1993) and orbital cycles (Ding et al. 1994; Liu et al. 1995) is also frequently used for the construction of timescales. In previous studies (Kukla 1987; Liu et al. 1995), soil SO was correlated with the deep-sea oxygen isotope stage 1; loess L1 was correlated with isotope stages 2, 3 and 4, the weak soil complex (L1SS1) with stage 3, and the S1 soil with stage 5. Absolute dating confirms this pattern of correlation (Fig. 3) except for the lower boundary of the soil complex LlSSl in the Malan loess: most of the TL dating yielded ages centered at -50 ka, which is significantly younger than the age of stage 3 (-59 ka) according to Martinson et al. (1987). The TL age is, however, in good agreement with the oxygen isotope age of ~ 50 ka provided by the eolian dust record in the North Pacific (Hovan et al. 1989), which represents a direct link between the Chinese loess and marine $\delta^{18}O$ records.

Another method of dating loess is Kukla抯 magnetic susceptibility model (Kukla et al. 1988; Kukla and An 1989), which assumes a constant deposition rate for magnetic minerals and calculates a time scale based on sediment thickness, weighted by susceptibility, by interpolation between two known age controls. Kukla抯 assumptions have been contested by some rock magnetic studies (Zhou et al. 1990; Heller et al. 1993; Verosub et al. 1993), which suggest a pedogenic-dominant origin of magnetic minerals. The results of the model, however, (Kukla et al. 1988; An et al. 1991) have demonstrated that it is a valuable working model, and is better than the one which assumes a constant eolian dust accumulation rate between the control ages, because the susceptibility signal, whatever its origin, is generally in inverse proportion to the sedimentation rate (Kukla et al. 1988; Kukla and An 1989).

The Weinan section has so far been the best dated by both ^{14}C and TL (Liu et al. 1994), and is used here as a stratigraphic standard (Fig. 4). The TL results from this section are coherent with those from the other sections (Fig. 3) and the TL ages for the upper part of the Weinan section are also coherent with the ^{14}C ages.

We apply two methods to develop the timescales for this section. Firstly, we reject one apparently anomalous TL age at 11.05 m depth and use all the others (Fig. 4) to devise a time scale by polynomial regression (model A). Secondly, we carefully examine the dating results by calculating the accumulation rate (Fig. 4) to eliminate the obviously or possibly outlying dates. The second age model (model B) uses only the apparently reliable age controls, interpolated by the susceptibility age model (Kukla and An 1989). The ages for the portion of the L2 loess below the lowest TL sample are extrapolated, assuming a sedimentation rate comparable to the L1 loess. The two age/depth models are generally consistent with the maximum difference of ~ 5.8 ka at 5.84 m depth, and ~ 8.9 ka at 10.84 m depth (Fig. 4). Model B is considered to be superior to model A because: (1) model B uses only the most reliable

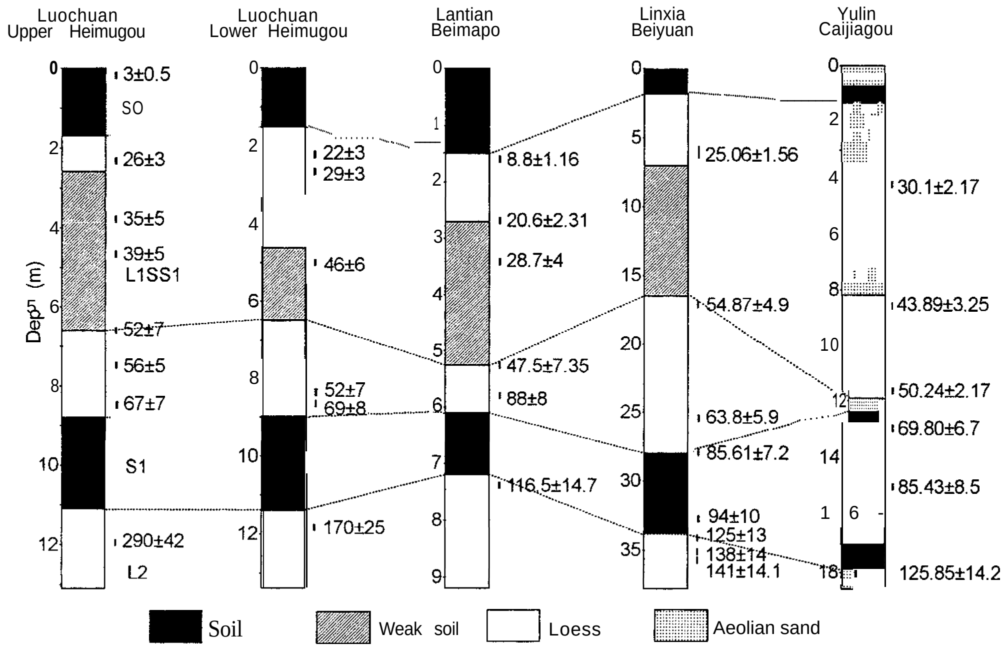

Fig. 3. Thermoluminescence (TL) dating results of five loess sections with available magnetic susceptibility measurements. TL data for the Upper and Lower Heimugou (Luochuan) and magnetic susceptibility measurements on which stratigraphic boundaries are based are from Forman (1991). Data for Beimapo (Lantian, 34°10 惟, 109°19 亳) are from Lu et al. (1988), with magnetic susceptibility and stratigraphic boundaries given by An et al. (1991). Data for Beiyuan (Linxia, 35°37 惟, 103°12 亳) are from Kang (1990) (but see Fang et al. 1994 for English version) with stratigraphic boundaries and magnetic susceptibility given by An et al. (1991). Data for Caijiagou (Yulin, 38°20′N, 109°30 亳) are from Sun et al. (1995). The two loess layers interbedded in the aeolian sandy beds at Caijiagou may correspond to the two soils in the L1SS1 soil complex at Weinan according to the magnetic susceptibility results

dates; and (2) the interpolation by the susceptibility model takes into account the accumulation rate, and thus is probably more suitable than any other regression. Both the age models are in good agreement with the previously published chrono-stratigraphic approaches shown in Fig. 3 in the Loess Plateau region. The ages of the stratigraphic boundaries (S0/L1LL1, L1LL1/L1SS1, L1SS1/L1LL2, L1LL2/S1 and S1/L2) of the two age models for the Weinan section are used as control points to perform the depth-age transformations for the Luochuan and Yichuan sections using the susceptibility model. The time scales for Luochuan section are consistent with previously published TL measurements (Forman 1991).

4 Paleo-weathering sequences

The variations in paleo-weathering intensity in the three sections are shown in Fig. 5, showing, overall, much higher values in soils than in loess, which is consistent with the stratigraphies in the field and in Fig. 2. Some minor differences exist between the curves, which may be attributable, firstly, to local factors, and secondly, to the fact that the two indices are based on the analyses of different elements. We have analyzed both indices on the samples of the Luochuan section. The CIW index has a higher coherency with the stratigraphic changes, so that it may be better than the Fed/Fet ratio as an index of the weathering history of loess.

A striking feature of all three sections is a series of sub-fluctuations that are inlaid within these longer-term trends, which represent intervals of low weathering intensity within the L1 and L2 loesses (marked by shadowed zones in Fig. 5). They exist in the three sections at similar stratigraphic positions, and thus must be related to common climatic conditions. Since the average soil temperatures in the region are below 0癈 from late autumn to early spring under modern interglacial conditions (Institute of Soil Sciences 1978), the chemical weathering of loess mainly depends upon summer temperatures and precipitation, and/or on the dust accumulation rate in winter and spring. Consequently, high weathering intensity can be interpreted as an indication of strengthened summer monsoon and/or weakened winter monsoon, and lower weathering intensity indicates the reverse. The intervals of low weathering intensity (LW-1 through LW-8) therefore indicate significant weakening of the summer monsoon and/or strengthening of winter monsoon. These fluctuations have no significant signals in magnetic susceptibility (Fig. 2) for which the cause is unknown.

In the Malan loess (L1), the six intervals of low weathering intensity values (LW-1 through LW-6) can be identified in all the three sections with the first two more clearly expressed in the Luochuan section. Another notable aspect is that most of them occur at or

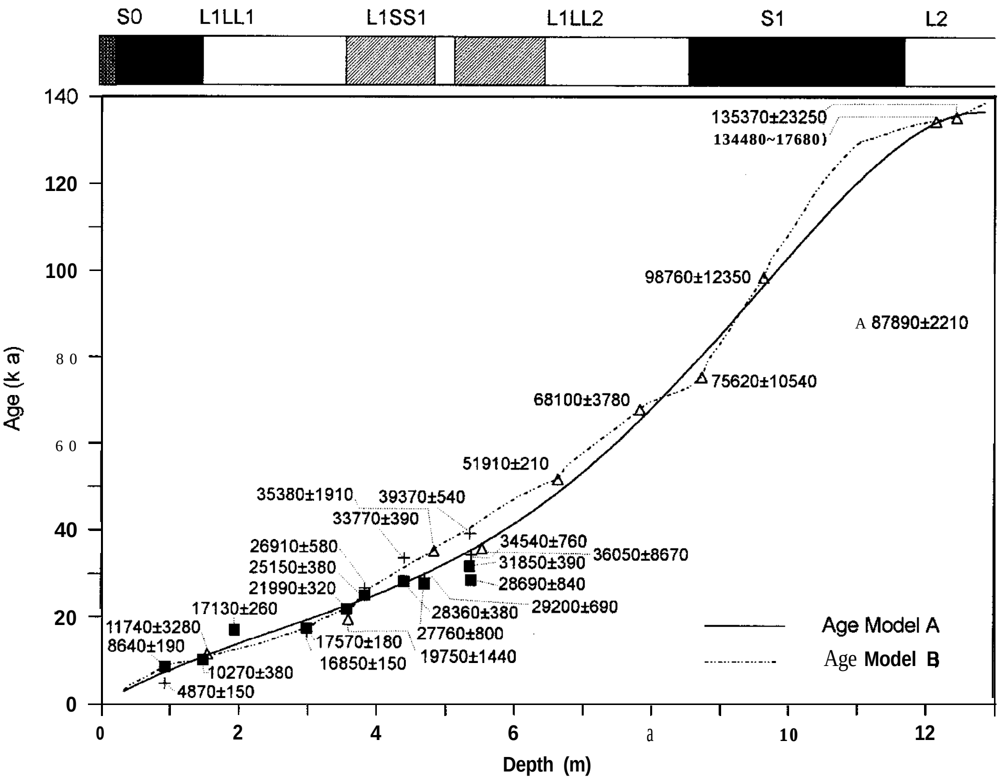

Fig. 4. Depth-age relationships of the Weinan section. All absolute dating results are from Liu et al. (1994). *Blac* ***squares*** are radiocarbon ages of humins; ***plus signs*** are radiocarbon ages of humic acid; *triangles* are TL ages. Liu et al. (1994) recommend the higher quality ages measured on humins because of their more stable chemical properties. Controversy with depth appears for radiocarbon ages older than 26000 years. The TL age at 11.05 m depth is anomalously young compared with the surrounding samples. Calculation based on the absolute ages gives an average accumulation rate of 6.7 cm/ka for the 1.49-1.95 m interval; 238.6 cm/ka years for the 1.95-3.0 m interval; 97 cm/ka for the 4.85-5.5 m interval and 7.25 cm/ka for 5.50-6.65 m interval, suggesting that the ^{14}C date of 17130± 260 on humins at 1.95 m depth may be too old and that of the TL date of 35380± 1910 at 4.85 m depth may be too young. Model A (*continuous* line) is developed by a polynomial regression on the absolute dating results after rejecting the anomalous TL date at 11.05 m depth. The ***fitted*** *curve* is a fifth-order polynomial: $Y=84.93X-8.99*10^{-2}X^2+1.76*10^{-5}X^3+2.31*10^{-7}X^4-1.40*10^{-10}X^5+63.14$ ($R^2=0.9932$, coefficient of determination $=0.9966$, standard error of the estimate $=3166.43$). Model B ***(dotted line)*** is constructed using the susceptibility age model of Kukla et al. (1988), and using the ^{14}C dates on humins and thermoluminescence measurements as control points in rejecting the possibly anomalous ^{14}C date at 1.95 m, TL dates at 4.85 m and 11.05 m, and the ^{14}C dates>26000 years. The ***legend*** of the stratigraphic units is the same as in Fig. 2

near the transitional boundaries between soil and loess units. The LW-1, LW-2, LW-5, LW-6 and LW-7 intervals are located, respectively, at or near the transitional boundaries S0/L1LL1, L1LL1/L1SS1, L1SS1/L1LL2, L1LL2/S1 and S1/L2. At Weinan, the LW-4 interval covers the thin, weathered loess layers within the LlSSl soil complex. The LW-8 peak at Yichuan is located just above the upper boundary of a weak soil visible in the field. Only the LW-3 interval is an exception as it lies entirely within the soil unit LlSSl and not near a soil/loess boundary. The identification of these low weathering intervals is also confirmed by an independent micromorphological study (Guo 1990) of the Malan loess at the Xifeng section (35°42 惟 , 107°36 扈), in which five horizons are revealed with fragmented microstructure and a striking decrease in indications of biological activity. The fragmented microstructure has been interpreted as a result of cryogenic processes, and the weak biological activity evidences the quasi-absence of vegetative cover (Guo 1990). These horizons at Xifeng are located respectively near the transitional boundaries S1/L1LL1, L1LL1/L1SS1, L1SS1/L1LL2, L1LL2/S1 and S1/L2, and are thus at stratigraphic levels similar to the LW-1, LW-2, LW-5, LW-6 and LW-7 low weathering intervals of this study.

The ages of the LW intervals on both model A and B timescales are given in Table 1. Spectral analysis of the Weinan CIW sequence (calculated on model B ages) (Fig. 6) reveals a strong -20 ka period (0.05 cycle/ka frequency) attributable to precessional forcing (Berger 1989), suggesting the validity of the time scales used. The model B ages for the Weinan section date the first seven low weathering intensity events at ~ 14, -21, -29, -38, -52, -71, and 135 ka BP, respectively, with minor differences amongst it and the other two sections. The differences are within the possible errors of susceptibility- and lithology-based stratigraphic correlation. Linear correlations of the four weathering curves plotted on the model B ages yield the correla-

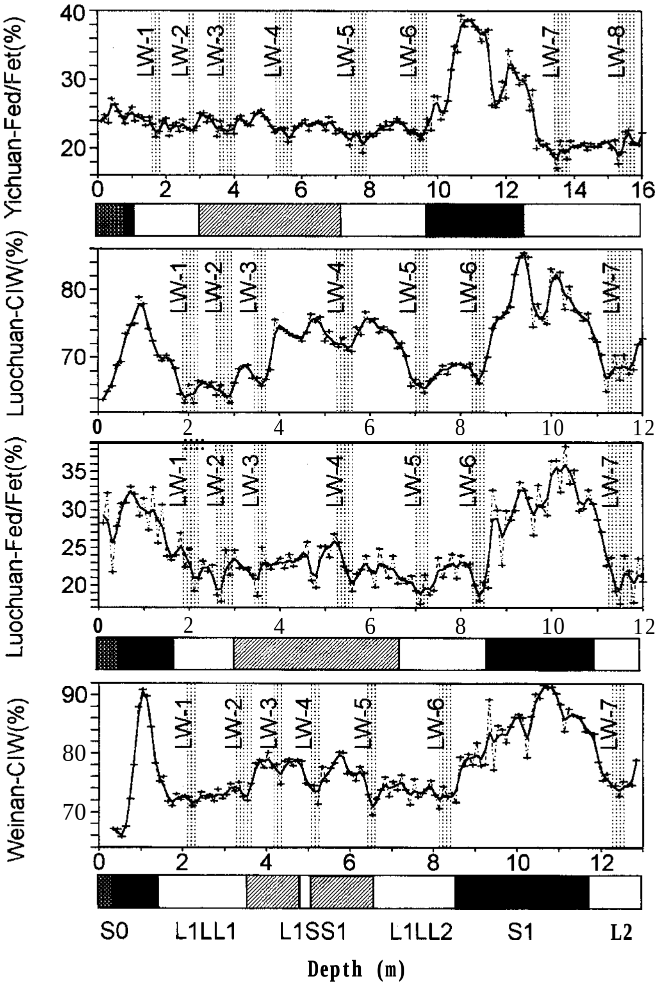

Fig. 5. Chemical weathering indices (CIW and Fed/Fet ratio) in the studied sections. The intervals of lower weathering intensity (*LW*) are *numbered* and *marked* by *shadowed zones*. The *dotted lines* through the *plus signs* are raw data and *continuous lines* are the smoothed data using a two-point moving average function. The *legend* of the stratigraphic units is the same as in Fig. 2

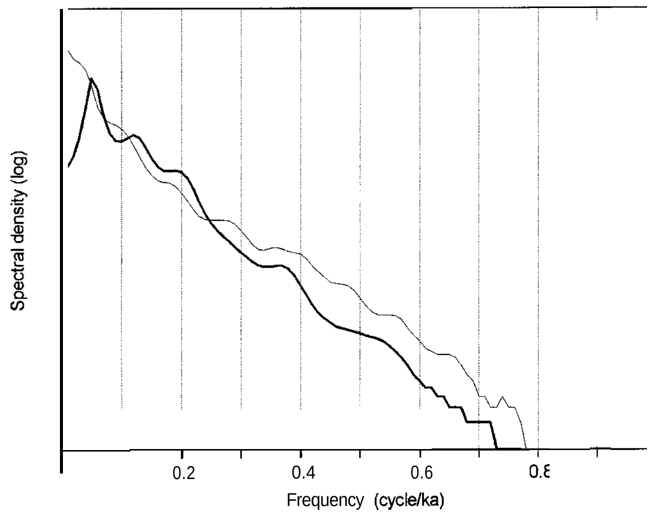

Fig. 6. Spectral analyses of the Weinan CIW time series (non-smoothed data plotted on model B ages). The analysis is performed using the maximum entropy method (Burg 1967). As the time series is too short for analyzing longer cycles, periods > 30 ka have been removed using a digital filter. The *thick curve* (logarithmic scale) represents the spectral density and the *fine curve* (logarithmic scale) represents the 95% confidence limit

tion coefficients (R) of **0.71** between the Luochuan CIW and the Weinan CIW, 0.82 between the Luochuan CIW and the Luochuan Fed/Fet, 0.80 between the Luochuan CIW and the Yichuan Fed/Fed, 0.71 between the Weinan CIW and Yichuan Fed/Fet, 0.65 between the Weinan CIW and the Yichuan Fed/Fet, 0.76 between the Luochuan Fed/Fet and the Yichuan Fed/Fet. In progressively dislocating the data between the two analyzed series, the coefficients decrease. These suggest that the four curves are generally coherent.

5 The China-North Atlantic link

Although the ultimate causes of the climatic events reflected by the LW intervals remain enigmatic, the ages of the first six LW intervals in the Malan loess (L1),

Table 1. Comparative ages of low weathering events (LW) identified by CIW and Fed/Fet weathering indices in Chinese loess sections and Heinrich events in the North Atlantic. Chronology of Heinrich layers in the North Atlantic DSDP 609 site is from Bond et al. (1992). Later ^{14}C measurements in V23-81 and V30-101 cores revised the age estimates for Heinrich events 3 and 4 from 28 to 27 ka BP and from 41 to 35.5 ka, respectively (Bond et al. 1993)

LW Events	Weinan		Louchuan		Yichuan		Heinrich layers in DSDP 609 site	
	Model A	Model B	Model A	Model B	Model A	Model B		
LW-1	14.7– 15.8	13.3– 14.1	12.7– 15.2	12.6– 14.6	13.4– 14.8	12.8– 14.2	H1	~ 14.3
LW-2	21.3– 22.5	20.4– 21.9	20.2– 23.4	19.5– 22.9	20.6– 23.2	20.0– 22.7	H2	-21.0
LW-3	26.1– 27.5	28.9– 30.8	26.9– 28.7	27.2– 29.3	25.6– 27.6	25.6– 28.0	H3	~ 28.0
LW-4	31.8– 35.2	36.9– 40.4	37.7– 41.0	40.2– 44.2	34.0– 36.5	35.7– 38.8	H4	-41.0
LW-5	46.4– 50.0	50.6– 54.5	51.6– 55.3	54.5– 57.1	48.9– 53.6	52.5– 55.9	H5	~ 52.0
LW-6	70.4– 77.2	70.7– 73.2	68.9– 77.2	67.1– 73.2	70.6 73.9	68.4– 70.8	H6	~ 69.0
LW-7	135.3-136.5	135.1-137.9	132.8-135.2	134.7-137.1	134.4-136.2	136.3-138.1		
LW-8					141.6-145.2	143.5-147.1		

within the constraints of our time scales, are close to being synchronous with those of the prominent Heinrich layers (H1 to H6) in the North Atlantic basin (Table 1). The Heinrich layers are a series of strata, rich in ice-rafted, lithic fragments, poor in foraminifera, and which resulted from massive discharges of debris-laden icebergs into the North Atlantic (Heinrich 1988; Broecker et al. 1992; Bond et al. 1992, 1993). The Heinrich events were also marked by decreases in sea surface temperature and in salinity (Bond et al. 1992), and have been shown to have had global expression, as indicated by several terrestrial climate records (Grimm et al. 1993; Guiot et al. 1993; Broecker 1994; Lowell et al. 1995). A seventh Heinrich event may exist right at the termination of the penultimate glaciation in the North Atlantic (Broecker 1994), which may be correlated with the LW-7 low weathering intensity interval in the L2 loess (Fig. 5). No 8th Heinrich event has been reported in the North Atlantic which might correspond with the LW-8 interval in the penultimate glacial loess at Yichuan (Fig. 5). Although the LW-1 and LW-2 at Weinan and Yichuan are less clear than at Luochuan, a high resolution pollen record from the South China Sea (Zhujiang-Q4 Core, 22°22 惟, 115°25 悥) (Lü et al. 1991) indicates that significant cooling occurred at ∼13.9–∼14.7 ka BP and ∼20.6–∼22.9 ka BP which can be temporally correlated with our LW-1 and LW-2 intervals. Because the core is located on the continental shelf off the mouth of the Zhujiang River, the pollen data mainly reflect record of vegetation changes in the Zhujiang Basin in southern China where the climate is strongly controlled by the east Asian summer monsoon.

In comparison with the grain-size time series and the correlation pattern of Porter and An (1995), based on a sedimentation-age model, our three youngest low-weathering intervals seem to correlate well with the uppermost peaks in the time series of quartz median diameter (Porter and An 1995). However, in view of the dating difficulties of loess and the potential error ranges of our TL dates, the correlation pattern for the older events remains tentative, as has also been indicated by Porter and An (1995) for their grain-size data. Much tighter dating control is needed for correlating events that are at most only a few thousand years long.

If the events in the North Atlantic and those in China are, in fact, linked, as we believe, then our results, in parallel with the Luochuan grain-size data (Porter and An 1995), suggest that the Heinrich events were synchronous, and therefore related, to the East Asian monsoons, and, in particular, the winter monsoon. This is also consistent with evidence of the East Asian origin of the Last Glacial Maximum dust in the GISP2 ice core (Biscaye et al. 1996).

The driving mechanism of the Heinrich events remains a matter of debate (Broecker 1994) and the mechanism linking them climatically to the East Asian monsoon is still unclear. It has been proposed that the presence of the climatic signals in eastern Asia, synchronous with the North Atlantic Younger Dryas event, may require non-orbital, large-scale control, such as changes in atmospheric concentration of greenhouse gases (Gasse et al. 1991; Kudrass et al. 1991). It is also thought that the Luochuan grain-size variations may have been linked with the Heinrich events through the Asian winter monsoon and the westerlies (Porter and An 1995), and a direct link between Chinese loess and the North Atlantic basin has been established by transport of dust of Asian origin via what was probably a northern branch of the jet stream to Greenland and the GISP2 ice-core (Biscaye et al. 1996).

An outstanding question is whether or not the intensity of the Asian summer monsoon has changed in conjunction with the Heinrich events. In view of the clear signals of Heinrich events 1 and 2 in the Zhujiang Q4 core (Lü et al. 1991) where the climate is strongly controlled by the Asian summer monsoon, the summer monsoon may have also experienced synchronous changes. Other quantitative estimates of climates based on pollen records have been reported from the African monsoon zone (Bonnefille et al. 1992; Vincens et al. 1993) and have shown significant cooling events around 14, 21 and 27 ^{14}C-ka BP, temporally correlative with our LW-1, LW-2 and LW-3 intervals. The evidence of low CH_4 concentration (Chappellaz et al. 1993) during the Dansgaard-Oeschger cold events seems also to imply that these events were related to changes in tropical and subtropical climates. Thus, the general cooling (or/and drying) in the African-Asian monsoon zone combined with the grain size data from the Luochuan loess section (Porter and An 1995) and the pollen record in the South China Sea (Lü et al. 1991) seem to indicate that both summer and winter monsoons have experienced changes approximately synchronous with the Heinrich events.

The stratigraphic position of the LW intervals in the soil-loess sequences may be of potential importance for understanding the mechanism that drove these events. Since the formation of the paleosols over the last climatic cycle had a clear -20 ka periodicity (An et al. 1991; Liu et al. 1995) which is attributable to orbital precessional forcing. The occurrence of most of the LW intervals at or near the soil-loess boundaries seems to suggest an affinity of these events with the precessional cycles, although, for the moment, we can suggest no reasonable idea of why this is so.

6 Conclusions

Our study on three sections in the Loess Plateau shows that paleo-weathering indices of loess can be used as sensitive indicators of paleoclimatic changes. A series of cold and/or drier events, as indicated by the lower values of the weathering indices, have been documented in the loess of the last glacial periods, which can be temporally correlated with the North Atlantic Heinrich events. This link has also been reported by Porter and An (1995) based on grain-size data from the Luochuan loess section. The LW events, combined with the synchronous signals in the South China Sea

(Lü et al. 1991) and in the African monsoon belt (Bonnefille et al. 1992; Vincens et al. 1993) may suggest that both summer and winter monsoons have experienced high frequency changes approximately synchronous with the Heinrich events.

Our results also suggest that similar weathering signals exist in the loess of the penultimate glacial period (corresponding to marine $\delta^{18}O$ stage 6), for which corresponding Heinrich events are not well established or have not yet been found in the North Atlantic. Another phenomenon which may be of potential importance for understanding the mechanisms driving these events is the general occurrence of the LW intervals at or near the boundaries between the loess and the soil units, although much additional work is needed for understanding the cause of this occurrence.

Acknowledgements. This work was supported by the National Natural Science Foundation of China. The authors are grateful to J. L. De Beaulieu, J. C. Duplessy, N. Fedoroff, G. Kukla and N. Petit-Maire for helpful discussions, to P. Biscaye for a critical review and improvement of the English version of the manuscript. Z. T. Guo thanks N. Petit-Maire and J. L. De Beaulieu for the warm hospitality during his research visit in Marseille, France, and the exchange program between the French CNRS and the Chinese Academy of Sciences. Finally, we would like to thank Dr. D. Rousseau and an anonymous reviewer for valuable suggestions and critical review of the paper.

References

An ZS, Kukla G, Porter SC, Xiao JL (1991) Magnetic susceptibility evidence of monsoon variation on the loess plateau of central China during the last 130000 years. Quat Res 36:29–36

An ZS, Porter SC, Zhou WJ, Lu YC, Donahue DJ, Head MJ, Wu XH, Ren JZ, Zheng HB (1993) Episode of strengthened summer monsoon climate of Younger Dryas age on the loess Plateau of central China. Quat Res 39:45–54

Beer J, Shen CD, Heller F, Liu TS, Bonani G, Dittrich B, Suter M, Kubik PW (1993) 搼Be and magnetic susceptibility in Chinese loess. Geophys Res Lett 20:57–60

Berger A (1989) Pleistocene climatic variability at astronomical frequencies. Quat Int 2: 1-14

Biscaye PE, Grousset FE, Revel M, Van der Gaast S, Zielinski GA, Vaars A (1996) Asian provenance of last glacial maximum dust in the GISP2 ice core, summit, Greenland. J Geophys Res (submitted)

Bond G, Heinrich H, Broecker WS, Labeyrie L, McManus J, Andrews J, Huon S, Jantschik R, Clasen S, Simet C, Tedesco K, Klas M, Bonani G, Ivy S (1992) Evidence for massive discharges of icebergs into North Atlantic ocean during the last glacial period. Nature 360: 245-249

Bond G, Broecker WS, Johnson S, McManus J, Labeyrie L, Jouzel J, Bonani G (1993) Correlations between climate records from North Atlantic sediments and Greenland ice. Nature 365:143–147

Bonnefille R, Chalie F, Guiot J, Vincens A (1992) Quantitative estimates of full glacial temperatures in equatorial Africa from palynological data. Clim Dyn 6: 251-257

Broecker WG, Bond M, Klas M, Clark E, McManus J (1992) Origin of the Northern Atlantic抯 Heinrich Events. Clim Dyn 6:91–109

Broecker WS (1994) Massive iceberg discharges as triggers for global climate change. Nature 372 : 421424

Burg JP (1967) Maximum entropy spectral analysis. 37th meeting Soc. Exploration Geophysicists, Oklahoma City, OK, USA

Chappellaz J, Blunier T, Raynaud D, Barnola JM, Schwander J, Stauffer B (1993) Synchronous changes in atmospheric CH4 and Greenland climate between 40 and 8 ky BP. Nature 366:443–445

Dansgaard W, Johnsen SJ, Clausen HB, Dahl-Jensen D, Gundestrup NS, Hammer CU, Hvidberg CS, Steffensen JP, Svelnbjornsdottir AE, Jouzel J, Bond G (1993) Evidence for general instability of past climate from a 250-ky ice-core record. Nature 364:218–220

Ding ZL, Yu ZW, Rutter NW, Liu TS (1994) Towards an orbital time scale for Chinese loess deposits. Quat Sci Rev 13:39-70

Duchaufour P (1983) Pédologie, Tome 1: Pédogenèse et Classification. Masson, Paris, pp l-477

Fang XM, Li JJ, Derbyshire E, Fritzpatrick EA, Kemp RA (1994) Micromorphology of the Beiyuan loess-paleosol sequence in Gansu Province, China: geomorphological and palaoenvironmental significance. Palaeogeogr, Palaeoclim, Palaeoecol 111: 289-303

Forman SL (1991) Late Pleistocene chronology of loess deposition near Luochuan, China. Quat Res 36: 19-28

Gasse F, Arnold M, Fontes JC, Fort M, Gilbert E, Huc A, Li BY, Li YF, Liu Q, Melieres F, Van Campo E, Wang FB, Zhang QS (1991) A 13000-year climate record from western Tibet. Nature 353: 742-745

Grimm EC, Jacobson GL Jr, Watts WA, Hansen BCS, Maasch KA (1993) A 50000-year record of climate oscillations from Florida and its temporal correlation with the Heinrich events. Science 261: 198–200

Guiot J, De Beaulieu JL, Cheddadi R, David F, Ponel P, Reille M (1993) The climate in western Europe during the last Glacial/Interglacial cycle derived from pollen and insect remains. Palaeogeogr, Palaeoclim, Palaeoecol 103 : 73-93

Guo ZT (1990) Succession des paleosols et des loess du centre-ouest de la Chine: approche micromorphologique. Thesis of University Paris VI, France, pp l-266

Guo ZT, Fedoroff N, An ZS (1991) Genetic types of the Holocene soil and the Pleistocene paleosols in the Xifeng loess section in central China. in: Liu TS (ed) Loess, environment and global change, Science Press, Beijing, China, pp 93-111

Guo ZT, Ding ZL, Liu TS (1996) Pedosedimentary events in loess of China and Quaternary climatic cycles. Chin Sci Bull 41:56–59

Harnois L (1988) The CIW index: a new chemical index of weathering. Sediment Geol 55 : 319-322

Heinrich H (1988) Origin and consequences of cyclic ice rafting in the northeast Atlantic Ocean during the past 130000 years. Quat Res 29: 142-152

Heller F, Shen CD, Beer J, Liu XM, Liu TS, Bronger A, Suter M, Bonani, G (1993) Quantitative estimates of pedogenic ferromagnetic mineral formation in Chinese loess and palaeoclimatic implications. Earth Planet Sci Lett 114:385–390

Hovan SA, Rea DK, Pisias NG, Shackleton NJ (1989) A direct link between the China loess and marine $\delta^{18}O$ records: aeolian flux to the north Pacific. Nature 340:296–298

Institute of Soil Sciences, Academia Sinica (1978) Soils in China. Science Press, Beijing (in Chinese) pp l-560

Kang JC (1990) The glacial sequence, loess records and their relations with environmental changes in west China over the last 150000 years. Thesis University of Lanzhou (in Chinese) pp 1-117

Kudrass HR, Erlenkeuser H, Vollbrecht R, Weiss W (1991) Global nature of Younger Dryas cooling event inferred from oxygen isotope data from Sulu sea cores. Nature 349:406–409

Kukla G (1987) Loess stratigraphy in central China. Quat Sci Rev 6: 191-219

Kukla GJ, An ZS (1989) Loess stratigraphy in central China. Palaeogeogr, Palaeoclim, Palaeoecol72 : 203-225

Kukla G, Heller F, Liu XM, Xu TC, Liu TS, An ZS (1988) Pleistocene climates in China dated by magnetic susceptibility. Geology 16:811–814